World Academy of Science, Engineering and Technology
International Journal of Physical and Mathematical Sciences
Vol:1, No:6, 2007

Accurate Optical Flow Based on Spatiotemporal Gradient Constancy Assumption

Adam Rabcewicz

***Abstract*—**Variational methods for optical flow estimation are known for their excellent performance. The method proposed by Brox et al. [5] exemplifies the strength of that framework. It combines several concepts into single energy functional that is then minimized according to clear numerical procedure. In this paper we propose a modification of that algorithm starting from the spatiotemporal gradient constancy assumption. The numerical scheme allows to establish the connection between our model and the CLG(H) method introduced in [18]. Experimental evaluation carried out on synthetic sequences shows the significant superiority of the spatial variant of the proposed method. The comparison between methods for the real-world sequence is also enclosed.

***Keywords*—**optical flow, variational methods, gradient constancy assumption.

I. Introduction

Estimation of optical flow is one of the most challenging problems among all computer vision tasks. Variational techniques consist in minimization of the energy functional which represents the assumptions concerning constancy of some features in the sequence as well as smoothness of the resulting flow. They have a nice advantage over other approaches — thanks to regularizer in the energy they are able to estimate the optical flow at locations where an image information is not available.

The work by Brox et al. [5] is undoubtly a significant progress among variational techniques that have been invented recently. These authors have developed an algorithm that incorporates a number of ideas that arose over the years starting from the classical work by Horn and Schunck [11]. This includes: a preservation of motion boundaries ([9], [16], [3], [21]), a penalization of outliers in the data ([4], [10]), coarse-to-fine strategies ([4], [1], [14]), spatiotemporal regularizers ([15], [22]) and robustness with respect to illumination changes ([20], [19], [17]).

A theoretical clarity of this approach as well as its impressive results cause researches to make an effort to improve it. Bruhn and Weickert in [6] have refined the method by separate robustification of the data terms what leads to slightly smaller angular error of the results. Amiaz and Kiryati [2] have embedded the energy of the method within an active contour segmentation framework. They have showed that such segmented optical flow is much more accurate.

In this paper we present yet another modification of that algorithm. Our goal is to impose a *spatiotemporal* gradient constancy assumption upon the model. In order to deeply explore this kind of assumption, the brightness constancy condition has been given up in the functional. We show that with some special approximation of image derivatives this model leads to the data term of some nice form. This allows to establish a connection of our model with the CLG(H) method introduced in [18] and provokes a discussion on the motion tensors terminology.

Our paper is organized as follows. In the next section our variational model is introduced. The numerical scheme is then described in Section III. In Section IV the connection with the CLG(H) method is established and the notion of motion tensors is discussed. Section V reports the results of experimental evaluation. Finally, the last section contains short summary and some concepts for future research.

Faculty of Mathematics and Computer Science, Nicolaus Copernicus University, Toruń, email: adrab@mat.uni.torun.pl

II. Model

Let $f\colon \Omega\times[0,T]\to\mathbb{R}$ denote an image sequence (Gaussian presmoothed with parameter σ), where $\Omega\subset\mathbb{R}^2$ is a rectangular domain. We wish to determine the optical flow field $\mathbf{w}(t) := (u(t), v(t), 1)^T$, $u(t), v(t)\colon \Omega\to\mathbb{R}$ at fixed time t which matches objects in subsequent frames at times t and $t+1$.

We assume that spatiotemporal gradient $\nabla_3 f := (f_x, f_y, f_t)^T$ is unchanged while moving. This condition can be expressed as

$$\nabla_3 f(\mathbf{x}+\mathbf{w}) = \nabla_3 f(\mathbf{x}-\mathbf{w}). \tag{1}$$

where $\mathbf{x} := (x, y, t)$. Note that two non-consecutive frames are used in the formula (1). This is necessary to utilize the temporal constancy of gradient in the algorithm. It will be shown later that it uses, in fact, three successive frames to compute the optical flow field at time t. It can be regarded as the result flow for the two first or the two last frames.

Our model is based on the following energy functional:

$$E(\mathbf{w}) = \int_\Omega \Psi\left(\left|\nabla_3 f(\mathbf{x}+\mathbf{w}) - \nabla_3 f(\mathbf{x}-\mathbf{w})\right|^2\right) + \alpha\Psi\left(|\nabla\mathbf{w}|^2\right)\, dx\, dy. \tag{2}$$

Here $|\nabla\mathbf{w}|^2 := |\nabla u|^2 + |\nabla v|^2$ and the symbol ∇ denotes ∇_2 for the spatial variant and ∇_3 for the spatiotemporal one. In the latter case one should replace the symbol Ω with $\Omega\times[0,T]$ under the integral. The function Ψ is the modified L^1 norm, $\Psi(s^2) := \sqrt{s^2+\varepsilon^2}$.

The Euler-Lagrange equations corresponding to the energy (2) read as follows:

$$\Psi'\left((f_{xz})^2 + (f_{yz})^2 + (f_{tz})^2\right)(f_{xx}f_{xz} + f_{xy}f_{yz} + f_{xt}f_{tz}) - \alpha\,\mathrm{div}\left(\Psi'(|\nabla\mathbf{w}|^2)\nabla u\right) = 0,$$

$$\Psi'\left((f_{xz})^2 + (f_{yz})^2 + (f_{tz})^2\right)(f_{xy}f_{xz} + f_{yy}f_{yz} + f_{yt}f_{tz}) - \alpha\,\mathrm{div}\left(\Psi'(|\nabla\mathbf{w}|^2)\nabla v\right) = 0$$

with reflecting boundary conditions. Here we use the following abbreviations:

$$\begin{aligned}
f_{xx} &:= \partial_{xx} f(\mathbf{x}+\mathbf{w}) + \partial_{xx} f(\mathbf{x}-\mathbf{w}),\\
f_{xy} &:= \partial_{xy} f(\mathbf{x}+\mathbf{w}) + \partial_{xy} f(\mathbf{x}-\mathbf{w}),\\
f_{yy} &:= \partial_{yy} f(\mathbf{x}+\mathbf{w}) + \partial_{yy} f(\mathbf{x}-\mathbf{w}),\\
f_{xt} &:= \partial_{xt} f(\mathbf{x}+\mathbf{w}) + \partial_{xt} f(\mathbf{x}-\mathbf{w}),\\
f_{xz} &:= \partial_{x} f(\mathbf{x}+\mathbf{w}) - \partial_{x} f(\mathbf{x}-\mathbf{w}),\\
f_{yt} &:= \partial_{yt} f(\mathbf{x}+\mathbf{w}) + \partial_{yt} f(\mathbf{x}-\mathbf{w}),\\
f_{yz} &:= \partial_{y} f(\mathbf{x}+\mathbf{w}) - \partial_{y} f(\mathbf{x}-\mathbf{w}),\\
f_{tz} &:= \partial_{t} f(\mathbf{x}+\mathbf{w}) - \partial_{t} f(\mathbf{x}-\mathbf{w}).
\end{aligned} \tag{3}$$

Note that the subscript t denotes the temporal derivative in contrast to z, which appears in expressions that arise as differences and are sought to be minimized.

III. Numerical Approximation

We will follow the construction of the numerical scheme performed in ([5]). The first step is to introduce the fixed point iteration on $\mathbf{w}$. Denote by $\mathbf{w}^k = (u^k, v^k, 1)^T$ the solution of the system at the iteration step k and let f^k_{**} be the abbreviations defined in (3) for the variable $\mathbf{w}^k$. An implicit scheme for the smoothness term and a semi-implicit scheme for the data term have been applied. This gives the following system of equations at the iteration step $k+1$:

$$\begin{aligned}
&\Psi'\big((f^{k+1}_{xz})^2 + (f^{k+1}_{yz})^2 + (f^{k+1}_{tz})^2\big)\\
&\qquad\times\big(f^k_{xx} f^{k+1}_{xz} + f^k_{xy} f^{k+1}_{yz} + f^k_{xt} f^{k+1}_{tz}\big)\\
&\qquad-\alpha\,\mathrm{div}\,\big(\Psi'(|\nabla u^{k+1}|^2 + |\nabla v^{k+1}|^2)\nabla u^{k+1}\big) = 0,\\
&\Psi'\big((f^{k+1}_{xz})^2 + (f^{k+1}_{yz})^2 + (f^{k+1}_{tz})^2\big)\\
&\qquad\times\big(f^k_{xy} f^{k+1}_{xz} + f^k_{yy} f^{k+1}_{yz} + f^k_{yt} f^{k+1}_{tz}\big)\\
&\qquad-\alpha\,\mathrm{div}\,\big(\Psi'(|\nabla u^{k+1}|^2 + |\nabla v^{k+1}|^2)\nabla v^{k+1}\big) = 0.
\end{aligned} \tag{4}$$

Next stage is to remove the nonlinearity from components f^{k+1}_{*z} using Taylor expansions

$$\begin{aligned}
f_*(\mathbf{x}+\mathbf{w}^{k+1}) &= f_*(\mathbf{x}+\mathbf{w}^k)\\
&\quad + f_{*x}(\mathbf{x}+\mathbf{w}^k)du^k + f_{*y}(\mathbf{x}+\mathbf{w}^k)dv^k,\\
f_*(\mathbf{x}-\mathbf{w}^{k+1}) &= f_*(\mathbf{x}-\mathbf{w}^k)\\
&\quad - f_{*x}(\mathbf{x}-\mathbf{w}^k)du^k - f_{*y}(\mathbf{x}-\mathbf{w}^k)dv^k,
\end{aligned}$$

where the unknown iteration variable $\mathbf{w}^{k+1}$ was split into the known variable $\mathbf{w}^k$ and an unknown update $\mathbf{dw}^k := (du^k, dv^k, 1)$. Therefore

$$f^{k+1}_{*z} = f^k_{*z} + f^k_{*x}\,du^k + f^k_{*y}\,dv^k \tag{5}$$

and applying the notation

$$\begin{aligned}
(\Psi')^k_D &:= \Psi'\big((f^k_{xz} + f^k_{xx}\,du^k + f^k_{xy}\,dv^k)^2\\
&\qquad + (f^k_{yz} + f^k_{yx}\,du^k + f^k_{yy}\,dv^k)^2\\
&\qquad + (f^k_{tz} + f^k_{xt}\,du^k + f^k_{yt}\,dv^k)^2\big),\\
(\Psi')^k_S &:= \Psi'\big(|\nabla(u^k + du^k)|^2 + |\nabla(v^k + dv^k)|^2\big)
\end{aligned}$$

the system (4) can be written as

$$\begin{aligned}
&(\Psi')^k_D\Big(f^k_{xx}(f^k_{xz} + f^k_{xx}\,du^k + f^k_{xy}\,dv^k)\\
&\qquad + f^k_{xy}(f^k_{yz} + f^k_{yx}\,du^k + f^k_{yy}\,dv^k)\\
&\qquad + f^k_{xt}(f^k_{tz} + f^k_{xt}\,du^k + f^k_{yt}\,dv^k)\Big)\\
&\qquad - \alpha\,\mathrm{div}\,\big((\Psi')^k_S\nabla u^{k+1}\big) = 0,\\
&(\Psi')^k_D\Big(f^k_{xy}(f^k_{xz} + f^k_{xx}\,du^k + f^k_{xy}\,dv^k)\\
&\qquad + f^k_{yy}(f^k_{yz} + f^k_{yx}\,du^k + f^k_{yy}\,dv^k)\\
&\qquad + f^k_{yt}(f^k_{tz} + f^k_{xt}\,du^k + f^k_{yt}\,dv^k)\Big)\\
&\qquad - \alpha\,\mathrm{div}\,\big((\Psi')^k_S\nabla v^{k+1}\big) = 0.
\end{aligned} \tag{6}$$

In that way we have obtained the system of equations with respect to **dw**. However, it is still nonlinear due to components Ψ'_D and Ψ'_S. So, the last step consists in removing this nonlinearity by applying another, nested fixed point iteration loop. Let the superscript l denote the internal fixed point loop iterator. At each step we compute the iteration variable $\mathbf{dw}^{k,l+1}$ as the solution of the linear system

$$\begin{aligned}
&(\Psi')^{k,l}_D\Big(f^k_{xx}(f^k_{xz} + f^k_{xx}\,du^{k,l+1} + f^k_{xy}\,dv^{k,l+1})\\
&\qquad + f^k_{xy}(f^k_{yz} + f^k_{yx}\,du^{k,l+1} + f^k_{yy}\,dv^{k,l+1})\\
&\qquad + f^k_{xt}(f^k_{tz} + f^k_{xt}\,du^{k,l+1} + f^k_{yt}\,dv^{k,l+1})\Big)\\
&\qquad - \alpha\,\mathrm{div}\,\Big((\Psi')^{k,l}_S\nabla(u^k + du^{k,l+1}\Big) = 0,\\
&(\Psi')^{k,l}_D\Big(f^k_{xy}(f^k_{xz} + f^k_{xx}\,du^{k,l+1} + f^k_{xy}\,dv^{k,l+1})\\
&\qquad + f^k_{yy}(f^k_{yz} + f^k_{yx}\,du^{k,l+1} + f^k_{yy}\,dv^{k,l+1})\\
&\qquad + f^k_{yt}(f^k_{tz} + f^k_{xt}\,du^{k,l+1} + f^k_{yt}\,dv^{k,l+1})\Big)\\
&\qquad - \alpha\,\mathrm{div}\,\Big((\Psi')^{k,l}_S\nabla(v^k + dv^{k,l+1}\Big) = 0
\end{aligned} \tag{7}$$

with the initialization $\mathbf{dw}^{k,0} = 0$. Terms $f(\mathbf{x}+\mathbf{w}^k)$ and $f(\mathbf{x}-\mathbf{w}^k)$ are obtained by bilinear interpolation after finishing the outer iteration step at level k.

Remarks about discretization:

1) **Spatial derivatives f^k_{xx}, f^k_{xy}, f^k_{yy}.** They have been discretized using twice the sixth-order approximation of the first-order derivative given by the stencil $(-1, 9, -45, 0, 45, -9, 1)/60$.
2) **Differences f^k_{xz}, f^k_{yz}.** They are simply the differences of two first-order spatial derivatives which have been computed using the stencil from the Remark 1. One should note that such temporal difference is itself a (doubled) standard second-order approximation of the derivative.
3) **Spatiotemporal derivatives f^k_{xt}, f^k_{yt}.** First we have discretized the temporal derivative of $\partial_{*t} f(\mathbf{x}+\mathbf{w}^k)$ using the first-order forward difference and of $\partial_{*t} f(\mathbf{x}-\mathbf{w}^k)$ using the backward difference, i.e:

$$\begin{aligned}
\partial_{*t} f(\mathbf{x}+\mathbf{w}^k) &= \partial_* f(\mathbf{x}+\mathbf{w}^k) - \partial_* f(\mathbf{x}),\\
\partial_{*t} f(\mathbf{x}-\mathbf{w}^k) &= \partial_* f(\mathbf{x}) - \partial_* f(\mathbf{x}-\mathbf{w}^k).
\end{aligned}$$

By substitution of the above in the definitions of f^k_{*t} we show that, in practise, $f^k_{*t} = f^k_{*z}$.

4) **Temporal derivative f^k_{tz}.** Similar procedure applied to f^k_{tz} gives the standard second-order central difference

$$f^k_{tz} = f(\mathbf{x} + \mathbf{w}^k) + f(\mathbf{x} - \mathbf{w}^k) - 2f(\mathbf{x}).$$

One should note that here we utilize the data from the middle frame which does not occur in the energy of the model.

Using these remarks one can discretize the system (7) with finite differences. This leads to a sparse linear system that can be solved using common numerical methods, e.g. SOR.

IV. Second-order motion tensor

A. The CLG(H) method

The CLG(H) method [18] is the first variational method for optical flow estimation which employs the spatiotemporal gradient constancy assumption. The key observation was that

$$((\nabla_3 f_x)^T \mathbf{w})^2 + ((\nabla_3 f_y)^T \mathbf{w})^2 + ((\nabla_3 f_t)^T \mathbf{w})^2 = \mathbf{w}^T H^2 \mathbf{w}, \tag{8}$$

where H denotes the Hessian matrix of f. The left hand side of (8) arises by embedding the result of the linearization of the gradient constancy condition (1) into a variational framework.

The CLG(H) energy functional is the following:

$$E_{CLG(H)}(\mathbf{w}) = \int_\Omega (\Psi(\mathbf{w}^T H^2_\rho \mathbf{w}) + \alpha\, \Psi(|\nabla \mathbf{w}|^2))\, dx\, dy.$$

Here $H^2_\rho = (K_\rho * H)^2$. The convolution H with a Gaussian kernel K_ρ was introduced to impose some local gradient constancy assumption.

This technique is itself a modification of the CLG method proposed by Bruhn et al. [8] which bases on the brightness constancy assumption. Formally functionals differ only in the matrix in the data term — there is a structure tensor J_ρ in CLG instead of H^2_ρ. What is interesting is that in spite of fundamental model differences they have the same elegant form.

B. Connection between the new technique and the CLG(H) method

Equation (5) can be written as

$$f^{k+1}_{*z} = (\mathbf{dw}^k)^T \nabla f^k_*.$$

Thus the expression inside $(\Psi')^k_D$ has the form

$$\begin{aligned}(f^{k+1}_{xz})^2 + (f^{k+1}_{yz})^2 + (f^{k+1}_{tz})^2 \\ = ((\mathbf{dw}^k)^T \nabla f^k_x)^2 + ((\mathbf{dw}^k)^T \nabla f^k_y)^2 + ((\mathbf{dw}^k)^T \nabla f^k_t)^2 \\ = (\mathbf{dw}^k)^T (H^k)^2 \mathbf{dw}^k.\end{aligned}$$

The last equality follows from (8) and it is true modulo distinguishing the t-derivatives and the z-differences. However, this identification is acceptable thanks to Remarks 2, 3 and 4.

Denote by (h_{ij}) elements of the matrix H^2. The equations (6) can be rewritten as

$$\begin{aligned}\Psi'((\mathbf{dw}^k)^T (H^k)^2 \mathbf{dw}^k)\Big(h_{11}\, du^k + h_{12}\, dv^k + h_{13}\Big) \\ - \alpha\, \mathrm{div}\left(\Psi'(|\nabla \mathbf{w}^{k+1}|^2) \nabla u^{k+1}\right) = 0, \\ \Psi'((\mathbf{dw}^k)^T (H^k)^2 \mathbf{dw}^k)\Big(h_{12}\, du^k + h_{22}\, dv^k + h_{23}\Big) \\ - \alpha\, \mathrm{div}\left(\Psi'(|\nabla \mathbf{w}^{k+1}|^2) \nabla v^{k+1}\right) = 0.\end{aligned} \tag{9}$$

Now it can be easily seen that the system (9) (and thus (6)) is nothing else than Euler-Lagrange equations for the functional

$$E(\mathbf{dw}^k) = \int_\Omega (\Psi((\mathbf{dw}^k)^T (H^k)^2 \mathbf{dw}^k) + \alpha\, \Psi(|\nabla \mathbf{w}^k|^2))\, dx\, dy.$$

Our algorithm solves the problem of minimizing the CLG(H) functional with respect to **dw** at each outer fixed point iteration step.

C. Motion tensors

Bruhn et al. in [7] introduce the terms *motion tensors* for both brightness and spatial gradient constancy assumptions. They are given by

$$\widetilde{J} = \widetilde{\nabla_3} f \widetilde{\nabla_3} f^T, \tag{10}$$

and

$$\widetilde{G} = \widetilde{\nabla_3} f_x \widetilde{\nabla_3} f_x^T + \widetilde{\nabla_3} f_y \widetilde{\nabla_3} f_y^T, \tag{11}$$

respectively, where $\widetilde{\nabla_3}$ denotes a variant of the ∇_3 operator with the temporal difference as the third component. As we have shown, this distinction can be abandoned at the implementation level, if only we treat the difference as an approximation of the derivative. This permits us to introduce a unified notation also for methods which start with linearized constancy assumptions. Thus we have:

- **First-order motion tensor J_ρ.** It is a consequence of the gray level constancy assumption and is given by $J_\rho = K_\rho * (\nabla_3 f \nabla_3 f^T)$. The more general form than (10) with a Gaussian convolution allows for taking into account methods which impose some local constancy conditions such as the classical one by Lucas and Kanade [12]. See also [8].
- **Second-order motion tensor H^2_ρ.** As we have shown, the spatiotemporal gradient constancy assumption leads to the H^2 tensor. It has more concise form than the G tensor from (11). In analogy to the J_ρ it is possible to integrate some local conditions by convolution with a Gaussian kernel [18].

V. Experimental Results

The quantitive evaluation has been carried out on the same synthetic sequences as in [5] to make a direct comparison between the original and modified methods. This include the most popular benchmark *Yosemite* with clouds and its variant without the sky. The former, created by Lynn Quam, combines the divergent motion of the mountains with the translational motion of the clouds with changing illumination. This region is well-known to create large angular errors in

many optical flow methods thus a number of authors have used the latter sequence where the cloudy region has been removed. It is available at `http://www.cs.brown.edu/~black/images.html`.

In our experiments we have set the number of outer loop steps to 40. We have found that, in our case, more iterations are needed than suggested in [5] for the two inner loops to get convergence . So, we have set the number of the inner iteration steps to 32 and the SOR steps to 8. The presmoothing parameter σ and the weight parameter α have been optimized.

The comparison between the methods has been made in Table I. We have observed that increasing the η parameter allows to obtain even more accurate results. Just to see it, Table I includes also the results for $\eta = 0.99$.

As we can see our method gives significantly better results for the *Yosemite with clouds* sequence. In case of non-cloudy version we get slightly better result with the 2D variant and much worse with the 3D variant. What is suprising, there is almost no difference between the spatial and spatiotemporal results. In fact, this difference is also quite slight in case of the first sequence. It can be explained as a side-effect

TABLE I
COMPARISON BETWEEN THE ORIGINAL AND THE MODIFIED METHOD USING VARIOUS SEQUENCES.

	Yosemite with clouds		Yosemite without clouds	
Method	AAE	STD	AAE	STD
Original (2D)	2.40°	6.90°	1.64°	1.43°
Modified (2D)	1.94°	5.35°	1.62°	1.57°
Modified (2D, $\eta = 0.99$)	1.79°	5.24°	1.54°	1.53°
Original (3D)	1.78°	7.00°	0.98°	1.17°
Modified (3D)	1.69°	5.23°	1.61°	1.53°
Modified (3D, $\eta = 0.99$)	1.59°	5.28°	1.54°	1.52°

of the specific construction of our model where the data term contains two non-consecutive frames. This is not well supported by the spatiotemporal regularization which prefers soft temporal transitions of the data. So, although the 3D result for Yosemite with clouds is still better from the original method, the non-cloudy variant reveals this drawback. We can conclude that our method works well in situations where only few frames are available. It seems to be appropriate in applications with a streaming data.

Table II shows a comparison of our results to several methods from the literature. As we can see, among 2D methods, the proposed one is outperformed only by the approach by Amiaz and Kiryati [2]. This is another modification of algorithm by Brox et al. and the idea of this technique can be applied to our model as well. This should give even better results and will be implemented in the future.

Results with the scaling factor $\eta = 0.99$ have been also enclosed in the table. One should note that they are non-comparative because the other results of corresponding methods have been obtained with $\eta = 0.95$. However, they are listed in order to show one another possibility of getting more accurate flow field.

This table also contains the result of the multiresolution variant of the CLG(H) method (Rabcewicz [18]). A more naive algorithm has been applied there – second-order derivatives have been computed directly at each warping level using suitable stencils and the spatial derivatives were computed using the middle frame. Section IV justifies that the proposed technique is the appropriate approach for that task. So, it is not suprising that it gives better results.

TABLE II
COMPARISON BETWEEN SEVERAL MODERN TECHNIQUES ON THE *Yosemite* SEQUENCE.

Method	AAE	STD
Horn-Schunck, modified [11]	9.78°	16.19°
Alvarez et al. [1]	5.53°	7.40°
Mémin-Pérez [13]	4.69°	6.89°
Bruhn et al. [8]	4.17°	7.72°
Brox et al. [5] (2D)	2.46°	7.31°
Bruhn-Weickert [6] (2D)	2.42°	6.70°
Rabcewicz [18]	2.28°	6.18°
Our method (2D)	**1.94°**	**5.35°**
Brox et al. [5] (3D)	1.94°	6.02°
Our method (2D, $\eta = 0.99$)	**1.79°**	**5.24°**
Bruhn-Weickert [6] (3D)	1.72°	6.88°
Our method (3D)	**1.69°**	**5.23°**
Amiaz-Kiryati [2]	1.64°	5.82°
Our method (3D, $\eta = 0.99$)	**1.59°**	**5.28°**

In our last experiment we use the real-world *Ettlinger Tor* sequence by Nagel. It is available at http://i21www.ira.uka.de/image_sequences/. In order to be able to make a qualitative comparison, the results of original and modified methods have been juxtaposed in Figure 1. The bottom left image depicts the magnitude of the optical flow field computed by Brox et al. It has been copied from the original work [5]. The bottom right shows the same but computed with the proposed method. We can see that both approaches give very good results in spite of interlacing artifacts that are present in all frames. However, some differences are visible. First, one can note that our algorithm suffers from the lack of the brightness assumption term. The flow corresponding to the bus is better estimated with the original technique. It is taking a bend, so the gradient constancy condition is not fulfilled. On the other hand, our approach has computed the motion flow more accurately at the background. It is solid and without any traces of the road lines. Its color is dark gray, not black as one could expected. This is a consequence of the fact that the background of the sequence is not static within these three frames. There is some motion – the camera moves slightly to the right and our model detected it correctly. Note also that the shapes of the vehicles are better matched with our method. It is clearly visible in case of two cars in the left side of the image. It seems that our algorithm does not suffer from the over-smoothing of flow discontinuities effect described in [2] as much as the original one.

VI. CONCLUSION AND FUTURE WORK

In this paper we have presented the algorithm for optical flow estimation which exploits the spatiotemporal gradient constancy. We have shown that this assumption even in non-linearized form leads to the tensor of elegant form H^2 which we have called the *second-order motion tensor*. Therefore it is the appropriate technique for implementing the multiresolution variant of the CLG(H) method [18]. Experimental evaluation

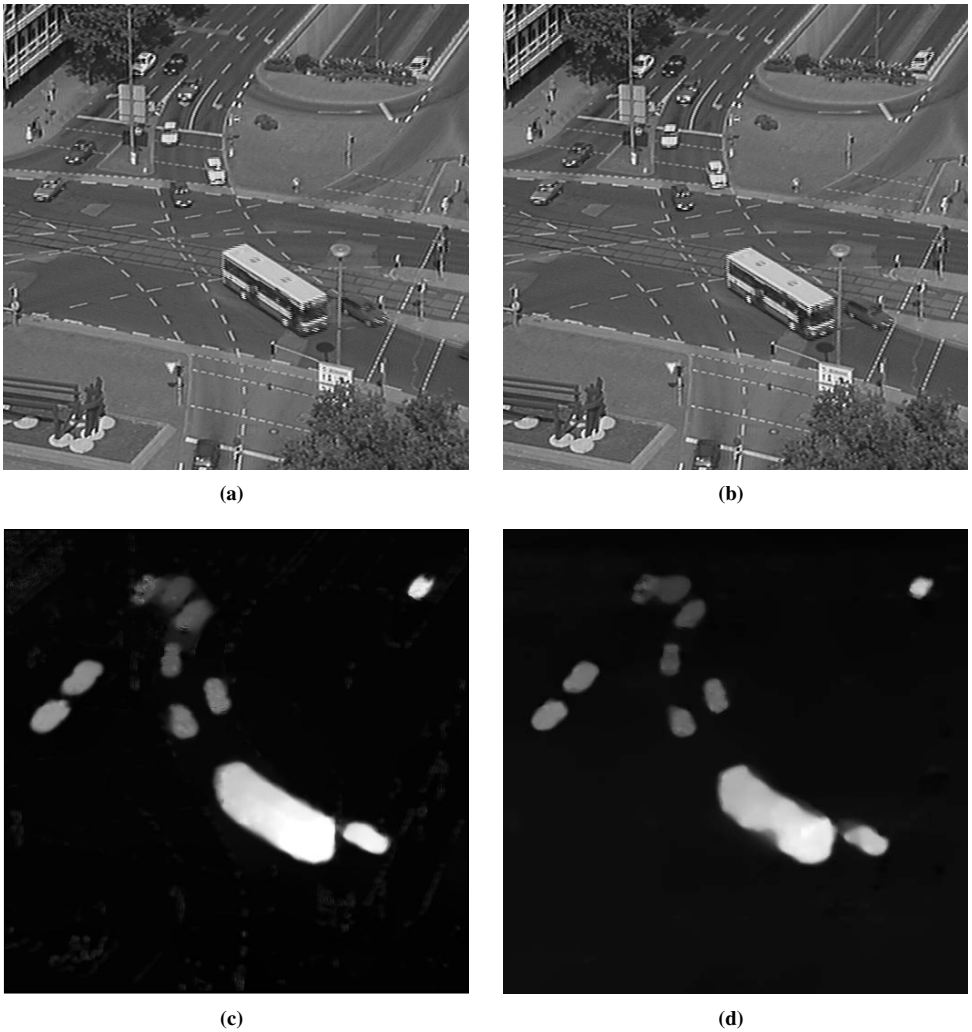

Fig. 1. (a) Frame 5 of the *Ettlinger Tor* sequence. (b) Frame 7. (c) Magnitude of the optical flow field computed between frame 5 and 6 with Brox et al.'s method. (d) Magnitude of the optical flow computed using frames 5, 6 and 7 with our method.

shows the superiority of our algorithm over the original one in case of spatial variants. Thus it is suitable for e.g. streaming data.

There are several possibilities to improve our algorithm basing on ideas from the literature:

- One can add the brightness constancy assumption to the model as in the original algorithm. This should help especially for sequences with irregular motions. It is interesting to compare the brightness constancy spreading on three frames, i.e. $f(\mathbf{x}+\mathbf{w}) - f(\mathbf{x}-\mathbf{w})$ with this from the model by Brox et al.
- We have already mention the Amiaz and Kiryati [2] algorithm. It combines the algorithm by Brox et al. with the idea of an active contour segmentation framework. This results in removing the over-smoothing of the optical flow at the discontinuities and, in consequence, gives much smaller angular error. This approach can be easily adopted to our model.
- Bruhn et al. [6] have developed an efficient numerical scheme for this kind of algorithms based on multigrid methods. Such a strategy can be also applied to our algorithm.

REFERENCES

[1] L. Alvarez, J. Weickert, and J. Sánchez. Reliable estimation of dense optical flow fields with large displacements. *International Journal of Computer Vision*, 39(1):41–56, August 2000.

[2] T. Amiaz and N. Kiryati. Piecewise-smooth dense optical flow via level sets. *International Journal of Computer Vision*, 68(2):111–124, June 2006.

[3] G. Aubert, R. Deriche, and P. Kornprobst. Computing optical flow via variational techniques. *SIAM Journal on Applied Mathematics*, 60(1):156–182, 1999.

[4] M. J. Black and P. Anandan. The robust estimation of multiple motions: Parametric and piecewise-smooth flow fields. *Computer Vision and Image Understanding*, 63(1):75–104, January 1996.

[5] T. Brox, A. Bruhn, N. Papenberg, and J. Weickert. High accuracy optical flow estimation based on a theory for warping. In T. Pajdla and J. Matas, editors, *Proceedings of the 8th European Conference on Computer Vision*, volume 3024 of *Lecture Notes in Computer Science*, pages 25–36, Prague, Czech Republic, 2004. Springer.

[6] A. Bruhn and J. Weickert. Towards ultimate motion estimation: Combining highest accuracy with real-time performance. In *Proc. Tenth International Conference on Computer Vision*, volume 1, pages 749–755, Beijing, China, June 2005. IEEE Computer Society.

[7] A. Bruhn, J. Weickert, T. Kohlberger, and C. Schnörr. A multigrid platform for real-time motion computation with discontinuity-preserving variational methods. *International Journal of Computer Vision*, 70(3):257–277, December 2006.

[8] A. Bruhn, J. Weickert, and C. Schnörr. Lucas/Kanade meets Horn/Schunck: Combining local and global optic flow methods. *International Journal of Computer Vision*, 61(3):211–231, February 2005.

[9] I. Cohen. Nonlinear variational method for optical flow computation. In *Proc. Eighth Scandinavian Conference on Image Analysis*, volume 1, pages 523–530, Tromso, Norway, May 1993.

[10] W. Hinterberger, O. Scherzer, C. Schnörr, and J. Weickert. Analysis of optical flow models in the framework of the calculus of variations. *Numerical Functional Analysis and Optimization*, 23(1/2):69–89, May 2002.

[11] B. Horn and B. Schunck. Determining optical flow. *Artificial Intelligence*, 17:185–203, August 1981.

[12] B. D. Lucas and T. Kanade. An iterative image registration technique with an application to stereo vision. In *Proc. Seventh International Joint Conference on Artificial Intelligence*, pages 674–679, Vancouver, Canada, August 1981.

[13] E. Mémin and P. Pérez. A multigrid approach for hierarchical motion estimation. In S. Chandran and U. Desai, editors, *Proc. Sixth International Conference on Computer Vision*, pages 933–938, Bombay, India, January 1998. Narosa Publishing House.

[14] E. Mémin and P. Pérez. Hierarchical estimation and segmentation of dense motion fields. *International Journal of Computer Vision*, 46(2):129–155, 2002.

[15] H.-H. Nagel. Extending the 'oriented smoothness constraint' into the temporal domain and the estimation of derivatives of optical flow. In O. D. Faugeras, editor, *ECCV'90*, volume 427 of *Lecture Notes in Computer Science*, pages 139–148. Springer, 1990.

[16] P. Nesi. Variational approach to optical-flow estimation managing discontinuities. *Image and Vision Computing*, 11(7):419–439, September 1993.

[17] M. Otte and H.-H. Nagel. Estimation of optical flow based on higher-order spatiotemporal derivatives in interlaced and non-interlaced image sequences. *Artificial Intelligence*, 78(1/2):5–43, November 1995.

[18] A. Rabcewicz. CLG method for optical flow estimation based on gradient constancy assumption. In X.-C. Tai, K.-A. Lie, T.F. Chan, and S. Osher, editors, *Image Processing Based on Partial Differential Equations: Proceedings of the International Conference on PDE-Based Image Processing and Related Inverse Problems, CMA, Oslo, Norway, August 8–12, 2005*, Mathematics and Visualization. Springer-Verlag, 2007.

[19] C. Schnörr. On functionals with greyvalue-controlled smoothness terms for determining optical flow. *IEEE Transactions on Pattern Analysis and Machine Intelligence*, 15(10):1074–1079, October 1993.

[20] S. Uras, F. Girosi, A. Verri, and V. Torre. A computational approach to motion perception. *Biological Cybernetics*, 60:79–87, 1988.

[21] J. Weickert and C. Schnörr. A theoretical framework for convex regularizers in PDE-based computation of image motion. *International Journal of Computer Vision*, 45(3):245–264, December 2001.

[22] J. Weickert and C. Schnörr. Variational optic flow computation with a spatio-temporal smoothness constraint. *Journal of Mathematical Imaging and Vision*, 14(3):245–255, May 2001.